The Zero Lower Bound and Estimation Accuracy
Online Appendix*

Tyler Atkinson   Alexander W. Richter   Nathaniel A. Throckmorton

ABSTRACT

This document contains the detrended equilibrium system and technical information about the solution and estimation methods. It also provides additional results, including supporting information about the bias in the price adjustment cost and habit persistence parameters, parameter estimates using datasets with shorter ZLB durations, estimates without misspecification, impulse responses to productivity growth and monetary policy shocks, filtered paths of the notional interest rate, statistics about our datasets, and estimates with government spending.

A DETRENDED EQUILIBRIUM SYSTEM

Medium-Scale Model The detrended system includes (1), (6), (7), (9), (16), (17) and

$$\tilde{y}_t = (v_t \tilde{k}_{t-1}/z_t)^\alpha n_t^{1-\alpha}, \tag{1}$$

$$r_t^k = \alpha m c_t z_t \tilde{y}_t/(v_t \tilde{k}_{t-1}), \tag{2}$$

$$\tilde{w}_t = (1-\alpha)m c_t \tilde{y}_t/n_t, \tag{3}$$

$$w_t^g = \pi_t z_t \tilde{w}_t/(\bar{\pi}\bar{z}\tilde{w}_{t-1}), \tag{4}$$

$$\tilde{y}_t^{gdp} = [1 - \varphi_p(\pi_t/\bar{\pi}-1)^2/2 - \varphi_w(w_t^g-1)^2/2]\tilde{y}_t - u_t\tilde{k}_{t-1}/z_t, \tag{5}$$

$$y_t^g = z_t \tilde{y}_t^{gdp}/(\bar{z}\tilde{y}_{t-1}^{gdp}), \tag{6}$$

$$\tilde{\lambda}_t = \tilde{c}_t - h\tilde{c}_{t-1}/z_t, \tag{7}$$

$$\tilde{w}_t^f = \chi n_t^\eta \tilde{\lambda}_t, \tag{8}$$

$$\tilde{c}_t + \tilde{x}_t = \tilde{y}_t, \tag{9}$$

$$x_t^g = z_t \tilde{x}_t/(\bar{z}\tilde{x}_{t-1}), \tag{10}$$

$$\tilde{k}_t = (1-\delta)(\tilde{k}_{t-1}/z_t) + \tilde{x}_t(1 - \nu(x_t^g-1)^2/2), \tag{11}$$

$$1 = \beta E_t[(\tilde{\lambda}_t/\tilde{\lambda}_{t+1})(s_t i_t/(z_{t+1}\pi_{t+1}))], \tag{12}$$

$$q_t = \beta E_t[(\tilde{\lambda}_t/\tilde{\lambda}_{t+1})(r_{t+1}^k v_{t+1} - u_{t+1} + (1-\delta)q_{t+1})/z_{t+1}], \tag{13}$$

$$1 = q_t[1 - \nu(x_t^g-1)^2/2 - \nu(x_t^g-1)x_t^g] + \beta\nu\bar{z}E_t[q_{t+1}(\tilde{\lambda}_t/\tilde{\lambda}_{t+1})(x_{t+1}^g)^2(x_{t+1}^g-1)/z_{t+1}], \tag{14}$$

$$\varphi_p(\pi_t/\bar{\pi}-1)(\pi_t/\bar{\pi}) = 1 - \theta_p + \theta_p m c_t + \beta\varphi_p E_t[(\tilde{\lambda}_t/\tilde{\lambda}_{t+1})(\pi_{t+1}/\bar{\pi}-1)(\pi_{t+1}/\bar{\pi})(\tilde{y}_{t+1}/\tilde{y}_t)], \tag{15}$$

$$\varphi_w(w_t^g-1)w_t^g = [(1-\theta_w)\tilde{w}_t + \theta_w\tilde{w}_t^f]n_t/\tilde{y}_t + \beta\varphi_w E_t[(\tilde{\lambda}_t/\tilde{\lambda}_{t+1})(w_{t+1}^g-1)w_{t+1}^g(\tilde{y}_{t+1}/\tilde{y}_t)]. \tag{16}$$

The variables are $\tilde{c}, n, \tilde{x}, \tilde{k}, \tilde{y}, \tilde{y}^{gdp}, u, v, w^g, x^g, y^g, \tilde{w}^f, \tilde{w}, r^k, \pi, i, i^n, q, mc, \tilde{\lambda}, z$, and s.

Small-Scale Model The detrended system includes (1), (7), (16), (17), (30), (31), (36), (39), and

$$\tilde{y}_t = n_t, \tag{17}$$

$$\tilde{w}_t = m c_t \tilde{y}_t/n_t, \tag{18}$$

$$\tilde{y}_t^{gdp} = [1 - \varphi_p(\pi_t/\bar{\pi}-1)^2/2]\tilde{y}_t, \tag{19}$$

$$\tilde{w}_t = \chi n_t^\eta \tilde{\lambda}_t, \tag{20}$$

$$\tilde{c}_t = \tilde{y}_t^{gdp}. \tag{21}$$

The variables are $\tilde{c}, n, \tilde{y}, \tilde{y}^{gdp}, y^g, \tilde{w}, \pi, i, i^n, mc, \tilde{\lambda}, z$, and s.

B NONLINEAR SOLUTION METHOD

We begin by compactly writing the detrended nonlinear equilibrium system as

$$E[f(\mathbf{s}_{t+1}, \mathbf{s}_t, \varepsilon_{t+1})|\mathbf{z}_t, \vartheta] = 0,$$

where f is a vector-valued function, $\mathbf{s}_t$ is a vector of variables, $\varepsilon_t \equiv [\varepsilon_{s,t}, \varepsilon_{z,t}, \varepsilon_{i,t}]'$ is a vector of shocks, $\mathbf{z}_t$ is a vector of states ($\mathbf{z}_t \equiv [\tilde{c}_{t-1}, i^n_{t-1}, \tilde{k}_{t-1}, \tilde{x}_{t-1}, \tilde{w}_{t-1}, s_t, z_t, \varepsilon_{i,t}]'$ for the model with capital and $\mathbf{z}_t \equiv [\tilde{c}_{t-1}, i^n_{t-1}, s_t, z_t, \varepsilon_{i,t}]'$ for the model without capital), and ϑ is a vector of parameters.

There are many ways to discretize the exogenous state variables, s_t, z_t, and $\varepsilon_{i,t}$. We use the Markov chain in Rouwenhorst (1995), which Kopecky and Suen (2010) show outperforms other methods for approximating autoregressive processes. The bounds on $\tilde{c}_{t-1}$, i^n_{t-1}, $\tilde{k}_{t-1}$, $\tilde{x}_{t-1}$, and $\tilde{w}_{t-1}$ are respectively set to $\pm 2.5\%$, $\pm 6\%$, $\pm 8\%$, $\pm 15\%$, $\pm 4\%$ of their deterministic steady state. These bounds were chosen so the grids contain 99.9% of the simulated values for each state variable and ZLB duration. We discretize the states into 7 evenly-spaced points, except for capital and the risk premium which use 11 and 13 points, respectively. The product of the points in each dimension, D, represents the total nodes in the state space ($D = 16{,}823{,}807$ for the model with capital and $D = 31{,}213$ for the model without capital). The realization of $\mathbf{z}_t$ on node d is denoted $\mathbf{z}_t(d)$. The Rouwenhorst method provides integration nodes, $[s_{t+1}(m), z_{t+1}(m), \varepsilon_{i,t+1}(m)]$, with weights, $\phi(m)$, for $m \in \{1, \ldots, M\}$. Since the exogenous variables evolve according to a Markov chain, the number of future realizations is the same as the state variables, $(13, 7, 7)$ or $M = 637$.

The vector of policy functions is denoted $\mathbf{pf}_t$ and the realization on node d is denoted $\mathbf{pf}_t(d)$ ($\mathbf{pf}_t \equiv [\tilde{c}_t(\mathbf{z}_t), \pi_t^{gap}(\mathbf{z}_t), n_t(\mathbf{z}_t), q_t(\mathbf{z}_t), v_t(\mathbf{z}_t)]$ for the capital model and $\mathbf{pf}_t \equiv [\tilde{c}_t(\mathbf{z}_t), \pi_t^{gap}(\mathbf{z}_t)]$ for the model without capital, where $\pi_t^{gap}(\mathbf{z}_t) \equiv \pi_t(\mathbf{z}_t)/\bar{\pi}$). Our choice of policy functions, while not unique, simplifies solving for the other variables in the nonlinear system of equations given $\mathbf{z}_t$.

The following steps outline our global policy function iteration algorithm:

1. Use Sims's (2002) `gensys` algorithm to solve the level-linear model without the ZLB constraint. Then map the solution to the discretized state space to initialize the policy functions.

2. On iteration $j \in \{1, 2, \ldots\}$ and each node $d \in \{1, \ldots, D\}$, use Chris Sims's `csolve` to find $\mathbf{pf}_t(d)$ to satisfy $E[f(\cdot)|\mathbf{z}_t(d), \vartheta] \approx 0$. Guess $\mathbf{pf}_t(d) = \mathbf{pf}_{j-1}(d)$. Then apply the following:

   (a) Solve for all variables dated at time t, given $\mathbf{pf}_t(d)$ and $\mathbf{z}_t(d)$.

   (b) Linearly interpolate the policy functions, $\mathbf{pf}_{j-1}$, at the updated state variables, $\mathbf{z}_{t+1}(m)$, to obtain $\mathbf{pf}_{t+1}(m)$ on every integration node, $m \in \{1, \ldots, M\}$.

   (c) Given $\{\mathbf{pf}_{t+1}(m)\}_{m=1}^{M}$, solve for the other elements of $\mathbf{s}_{t+1}(m)$ and compute

   $$\mathbb{E}[f(\mathbf{s}_{t+1}, \mathbf{s}_t(d), \varepsilon_{t+1})|\mathbf{z}_t(d), \vartheta] \approx \textstyle\sum_{m=1}^{M} \phi(m) f(\mathbf{s}_{t+1}(m), \mathbf{s}_t(d), \varepsilon_{t+1}(m)).$$

   When `csolve` converges, set $\mathbf{pf}_j(d) = \mathbf{pf}_t(d)$.

3. Repeat step 2 until $\text{maxdist}_j < 10^{-6}$, where $\text{maxdist}_j \equiv \max\{|\mathbf{pf}_j - \mathbf{pf}_{j-1}|\}$. When that criterion is satisfied, the algorithm has converged to an approximate nonlinear solution.

C ESTIMATION ALGORITHM

We use a random walk Metropolis-Hastings algorithm to estimate the model in section 3 with artificial data of 120 quarters. To measure how well the model fits the data, we use either the adapted particle filter described in Algorithm 14 in Herbst and Schorfheide (2016), which modifies the basic bootstrap filter in Stewart and McCarty (1992) and Gordon et al. (1993) to better account for the outliers in the data, or the inversion filter recently used by Guerrieri and Iacoviello (2017).

C.1 METROPOLIS-HASTINGS ALGORITHM   The following steps outline the algorithm:

1. Generate artificial data consisting of the output growth gap, the inflation rate, and the nominal interest rate, $\mathbf{x}_t \equiv [y_t^g, \pi_t, i_t]'$, where $N_x = 3$ is the number of observable variables.

2. Specify the prior distributions, means, variances, and bounds of each element of the vector of N_e estimated parameters, $\theta \equiv [\varphi_p, \phi_\pi, \phi_y, h, \rho_s, \rho_i, \sigma_z, \sigma_s, \sigma_i]'$.

3. Find the posterior mode to initialize the preliminary Metropolis-Hastings step.

   (a) For all $i \in \{1, \ldots, N_m\}$, where $N_m = 5{,}000$, apply the following steps:

      i. Draw $\hat{\theta}_i$ from the joint prior distribution and calculate its density value:
      $$\log \ell_i^{prior} = \sum_{j=1}^{N_e} \log p(\hat{\theta}_{i,j}|\mu_j, \sigma_j^2),$$
      where p is the prior density function of parameter j with mean μ_j and variance σ_j^2.

      ii. Solve the model given $\hat{\theta}_i$. Follow Appendix B for the nonlinear model and use OccBin for the PW linear model. Repeat 3(a)i if the algorithm does not converge.

      iii. Obtain the model log-likelihood, $\log \ell_i^{model}$. Apply the particle filter described in Appendix C.2 to the nonlinear model and the inversion filter to the PW linear model.

      iv. The posterior log-likelihood is $\log \ell_i^{post} = \log \ell_i^{prior} + \log \ell_i^{model}$

   (b) Calculate $\max(\log \ell_1^{post}, \ldots, \log \ell_{N_m}^{post})$ and find the corresponding parameter vector, $\hat{\theta}_0$.

4. Approximate the covariance matrix for the joint posterior distribution of the parameters, Σ, which is used to obtain candidate draws during the preliminary Metropolis-Hastings step.

   (a) Locate the draws with a likelihood in the top decile. Stack the $N_{m,sub} = (1-p)N_m$ draws in a $N_{m,sub} \times N_e$ matrix, $\hat{\Theta}$, and define $\tilde{\Theta} = \hat{\Theta} - \sum_{i=1}^{N_{m,sub}} \hat{\theta}_{i,j}/N_{m,sub}$.

   (b) Calculate $\Sigma = \tilde{\Theta}'\tilde{\Theta}/N_{m,sub}$ and verify it is positive definite, otherwise repeat step 3.

5. Perform an initial run of the random walk Metropolis-Hastings algorithm.

(a) For all $i \in \{0, \ldots, N_d\}$, where $N_d = 25{,}000$, perform the following steps:

    i. Draw a candidate vector of parameters, $\hat{\theta}_i^{cand}$, where

$$\hat{\theta}_i^{cand} \sim \begin{cases} \mathbb{N}(\hat{\theta}_0, c_0\Sigma) & \text{for } i = 0, \\ \mathbb{N}(\hat{\theta}_{i-1}, c\Sigma) & \text{for } i > 0. \end{cases}$$

    We set $c_0 = 0$ and tune c to target an overall acceptance rate of roughly 30%.

    ii. Calculate the prior density value, $\log \ell_i^{prior}$, of the candidate draw, $\hat{\theta}_i^{cand}$, as in 3(a)i.

    iii. Solve the model given $\hat{\theta}_i^{cand}$. If the algorithm does not converge repeat 5(a)i.

    iv. Obtain the model log-likelihood value, $\log \ell_i^{model}$, using the methods in 3(a)iii.

    v. Accept or reject the candidate draw according to

$$(\hat{\theta}_i, \log \ell_i) = \begin{cases} (\hat{\theta}_i^{cand}, \log \ell_i^{cand}) & \text{if } i = 0, \\ (\hat{\theta}_i^{cand}, \log \ell_i^{cand}) & \text{if } \min(1, \ell_i^{cand}/\ell_{i-1}) > \hat{u}, \\ (\hat{\theta}_{i-1}, \log \ell_{i-1}) & \text{otherwise,} \end{cases}$$

    where $\hat{u}$ is a draw from a uniform distribution, $\mathbb{U}[0, 1]$, and the posterior log-likelihood associated with the candidate draw is $\log \ell_i^{cand} = \log \ell_i^{prior} + \log \ell_i^{model}$.

(b) Burn the first $N_b = 5{,}000$ draws and use the remaining sample to calculate the mean draw, $\hat{\theta}^{5(b)} = \sum_{i=N_b+1}^{N_d} \hat{\theta}_i/(N_d - N_b)$, and the covariance matrix, $\Sigma^{5(b)}$. We follow step 4 to calculate $\Sigma^{5(b)}$ but use all $N_d - N_b$ draws instead of just the upper pth percentile.

6. Conduct a final run of the Metropolis-Hastings algorithm by repeating step 5, where $N_d = 50{,}000$, $\hat{\theta}_0 = \hat{\theta}^{5(b)}$, and $\Sigma = \Sigma^{5(b)}$. The final posterior mean estimates are $\hat{\theta} = \sum_{i=1}^{N_d} \hat{\theta}_i/N_d$.

C.2 ADAPTED PARTICLE FILTER   Henceforth, our definition of $\mathbf{s}_t$ from Appendix B is referred to as the state vector, which should not be confused with the state variables for the nonlinear model.

1. Initialize the filter by drawing $\{\varepsilon_{t,p}\}_{t=-24}^{0}$ for all $p \in \{0, \ldots, N_p\}$ and simulating the model, where N_p is the number of particles. We initialize the filter with the final state vector, $\mathbf{s}_{0,p}$, which is approximately a draw from the model's ergodic distribution. We set $N_p = 40{,}000$.

2. For $t \in \{1, \ldots, T\}$, sequentially filter the nonlinear model as follows:

(a) For $p \in \{1, \ldots, N_p\}$, draw shocks from an adapted distribution, $\varepsilon_{t,p} \sim \mathbb{N}(\bar{\varepsilon}_t, I)$, where $\bar{\varepsilon}_t$ maximizes $p(\xi_t|\mathbf{s}_t)p(\mathbf{s}_t|\bar{\mathbf{s}}_{t-1})$ and $\bar{\mathbf{s}}_{t-1} = \sum_{p=1}^{N_p} \mathbf{s}_{t-1,p}/N_p$ is the mean state vector.

    i. Use the model solution to update the state vector, $\mathbf{s}_t$, given $\bar{\mathbf{s}}_{t-1}$ and a guess for $\bar{\varepsilon}_t$. Define $\mathbf{s}_t^h \equiv H\mathbf{s}_t$, where H selects the observable variables from the state vector.

ii. Calculate the measurement error, $\xi_t = \mathbf{s}_t^h - \mathbf{x}_t$, which is assumed to be multivariate normally distributed, $p(\xi_t|\mathbf{s}_t) = (2\pi)^{-3/2}|R|^{-1/2}\exp(-\xi_t'R^{-1}\xi_t/2)$, where $R \equiv \text{diag}(\sigma_{me,y^g}^2, \sigma_{me,\pi}^2, \sigma_{me,i}^2)$ is a diagonal matrix of measurement error variances.

iii. The probability of observing the current state, $\mathbf{s}_t$, conditional on $\bar{\mathbf{s}}_{t-1}$, is given by

$$p(\mathbf{s}_t|\bar{\mathbf{s}}_{t-1}) = (2\pi)^{-3/2}\exp(-\bar{\varepsilon}_t'\bar{\varepsilon}_t/2).$$

iv. Maximize $p(\xi_t|\mathbf{s}_t)p(\mathbf{s}_t|\bar{\mathbf{s}}_{t-1}) \propto \exp(-\xi_t'R^{-1}\xi_t/2)\exp(-\bar{\varepsilon}_t'\bar{\varepsilon}_t/2)$ by solving for the optimal $\bar{\varepsilon}_t$. We use MATLAB's `fminsearch` routine converted to Fortran.

(b) Use the model solution to predict the state vector, $\mathbf{s}_{t,p}$, given $\mathbf{s}_{t-1,p}$ and $\varepsilon_{t,p}$.

(c) Calculate $\xi_{t,p} = \mathbf{s}_{t,p}^h - \mathbf{x}_t$. The unnormalized weight on particle p is given by

$$\omega_{t,p} = \frac{p(\xi_t|\mathbf{s}_{t,p})p(\mathbf{s}_{t,p}|\mathbf{s}_{t-1,p})}{g(\mathbf{s}_{t,p}|\mathbf{s}_{t-1,p},\mathbf{x}_t)} \propto \frac{\exp(-\xi_{t,p}'R^{-1}\xi_{t,p}/2)\exp(-\varepsilon_{t,p}'\varepsilon_{t,p}/2)}{\exp(-(\varepsilon_{t,p}-\bar{\varepsilon}_t)'(\varepsilon_{t,p}-\bar{\varepsilon}_t)/2)}.$$

Without adaptation, $\bar{\varepsilon}_t = 0$ and $\omega_{t,p} = p(\xi_t|\mathbf{s}_{t,p})$, as in a basic bootstrap particle filter. The time-t contribution to the model log-likelihood is $\ell_t^{model} = \sum_{p=1}^{N_p}\omega_{t,p}/N_p$.

(d) Normalize the weights, $W_{t,p} = \omega_{t,p}/\sum_{p=1}^{N_p}\omega_{t,p}$. Then use systematic resampling with replacement from the swarm of particles as described in Kitagawa (1996) to get a set of particles that represents the filter distribution and reshuffle $\{\mathbf{s}_{t,p}\}_{p=1}^{N_p}$ accordingly.

3. The model log-likelihood is $\log\ell^{model} = \sum_{t=1}^{T}\log\ell_t^{model}$.

Aruoba et al. (2018) apply the same methodology to a New Keynesian model with sunspot shocks. See Herbst and Schorfheide (2016) for a comprehensive discussion of the different particle filters.

D CONTINUOUS RANK PROBABILITY SCORE (CRPS) EXAMPLE

Figure 1 shows an example of the 8-quarter ahead forecast distribution of the nominal interest rate given the parameter estimates from NL-PF-5%. We picked a dataset where the ZLB binds for six quarters, from period 90 to 95 in the sample. The forecasts are initialized at the filtered state in period 89, immediately before the ZLB first binds, and the forecast distribution is approximated based on 10,000 simulations. Due to a strong tendency for the forecasts to revert to the stochastic steady state, the mean forecast for the nominal interest rate is 2.32%. However, the probability density function (PDF) in the left panel shows a significant number of forecasts remain near or at the ZLB, even after 8 quarters. The true realization equals 1.94%, which means there is significant probability mass under the PDF above and below the true value. The right panel shows the cumulative distribution function (CDF) of the forecasts. The CRPS for this dataset and estimation method is closely related to the shaded area, which has the same units as the forecasted variable.
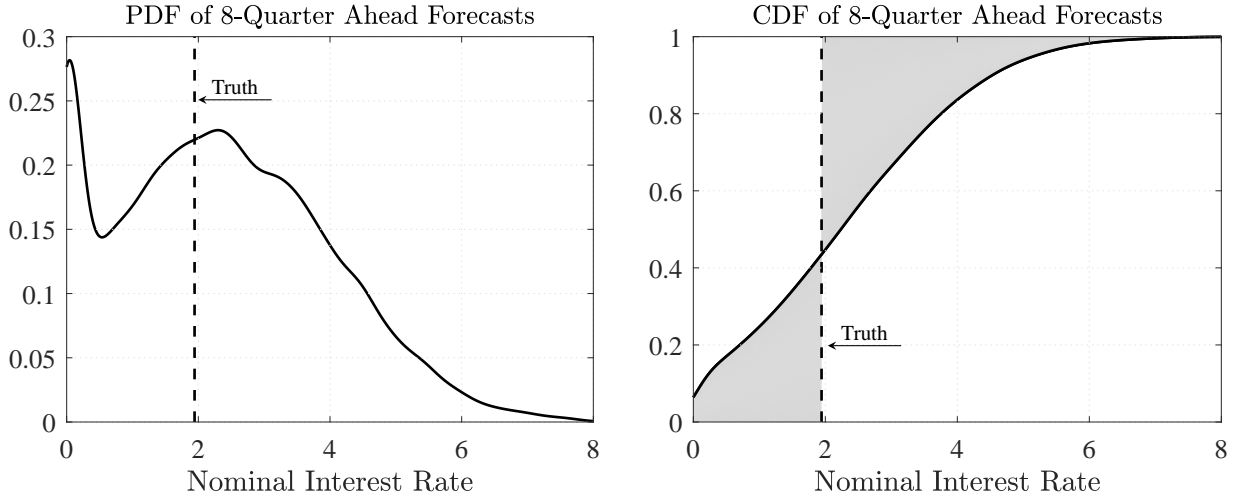
Figure 1: Example forecast distribution in the period before the ZLB binds in the data.

E ADDITIONAL RESULTS

First, we examine the sources of the bias in the estimates of the habit persistence and price adjustment cost parameters. Second, we report the parameter estimates for datasets with ZLB events between 0 and 30 quarters long. Third, we show how misspecification affects the parameter estimates and impulse responses using generated data from our small-scale model. Fourth, we plot impulse responses to a productivity growth and monetary policy shock when the ZLB binds. Fifth, we compare the filtered paths of the notional interest rate. Sixth, we provide additional statistics about the ZLB events in our datasets. Finally, we examine how government spending affects our results.

E.1 PRICE ADJUSTMENT COST AND HABIT PERSISTENCE   In table 4, estimates of the price adjustment cost (φ_p) and habit persistence (h) parameters have some of the largest NRMSEs, even in datasets without a ZLB event. These parameters are critical for output and inflation dynamics, so understanding the source of the bias is important for interpreting our results. The small-scale model lacks important shock amplifiers for output, such as sticky wages and variable capital utilization. Therefore, the response of output growth is too small when the model is parameterized with the true values. Conversely, the lack of sticky wages means marginal costs are overly volatile and inflation is too sensitive to shocks. If misspecification impacted the responses of output growth and inflation in the same direction, the estimated shock size would have been affected. Instead, estimates of h are lower than the true value, amplifying the response of output. Estimates of φ_p are biased upward, flattening the price Phillips curve and stabilizing inflation despite overly volatile marginal costs.

Another potentially important source of the bias is the misspecification in the aggregate resource constraint. Movements in wage adjustment costs, capital utilization costs and other terms could be interpreted as price adjustment costs through a larger estimate of φ_p. However, that is

6

unlikely to drive the bias in estimates of φ_p and h. The NL-PF-5% and Lin-KF-5% estimates of φ_p and h are very similar, despite the absence of price adjustment costs in the aggregate resource constraint in the linear model (i.e., $\hat{y}_t = \hat{y}_t^{gdp} = \hat{c}_t$). Therefore, the upward bias in φ_p is not the result of price adjustment costs absorbing the gap between consumption and output in the DGP.

The middle columns of table 5, where only sticky wages are added to the small-scale model, support these conclusions. In particular, in datasets without a ZLB event, there is virtually no bias in the OB-IF-0% estimates of φ_p and h, but there is a large upward bias in σ_s. When sticky wages are added, the volatility of output growth is still too small due to the absence of investment and capital utilization, but the volatility of inflation is now proportionally too small as well. σ_s increases to match the dynamics of the output and inflation data, while h and φ_p remain close to their true values. In the right two columns of table 5, the full model is estimated and σ_s is close to the truth.

Ptr	Truth	NL-PF-5%		OB-IF-0%		Lin-KF-5%	
		0Q	30Q	0Q	30Q	0Q	30Q
ρ_s	0.8	0.43 (0.37, 0.50) {0.47, 0.00}	0.52 (0.40, 0.68) {0.37, 0.04}	0.39 (0.31, 0.47) {0.52, 0.00}	0.44 (0.26, 0.71) {0.48, 0.04}	0.43 (0.35, 0.50) {0.47, 0.00}	0.55 (0.40, 0.77) {0.33, 0.12}
ρ_i	0.8	0.74 (0.69, 0.78) {0.09, 0.26}	0.75 (0.71, 0.81) {0.07, 0.52}	0.69 (0.65, 0.73) {0.15, 0.00}	0.68 (0.62, 0.73) {0.16, 0.00}	0.74 (0.70, 0.78) {0.09, 0.30}	0.79 (0.73, 0.84) {0.05, 0.86}
σ_z	0.005	0.0052 (0.0041, 0.0067) {0.17, 0.88}	0.0062 (0.0037, 0.0134) {0.54, 0.82}	0.0086 (0.0069, 0.0099) {0.73, 0.00}	0.0107 (0.0071, 0.0163) {1.28, 0.00}	0.0053 (0.0041, 0.0067) {0.17, 0.86}	0.0078 (0.0042, 0.0138) {0.83, 0.44}
σ_s	0.005	0.0166 (0.0139, 0.0212) {2.37, 0.00}	0.0196 (0.0113, 0.0261) {3.04, 0.12}	0.0183 (0.0143, 0.0230) {2.71, 0.00}	0.0239 (0.0085, 0.0355) {4.15, 0.04}	0.0169 (0.0141, 0.0216) {2.42, 0.00}	0.0169 (0.0065, 0.0257) {2.59, 0.12}
σ_i	0.002	0.0018 (0.0015, 0.0022) {0.13, 0.64}	0.0016 (0.0014, 0.0021) {0.21, 0.38}	0.0021 (0.0019, 0.0023) {0.09, 0.78}	0.0021 (0.0019, 0.0025) {0.11, 0.78}	0.0018 (0.0015, 0.0022) {0.13, 0.64}	0.0017 (0.0015, 0.0020) {0.16, 0.44}
ϕ_π	2.0	2.04 (1.81, 2.23) {0.07, 0.96}	2.03 (1.84, 2.33) {0.07, 0.90}	1.96 (1.70, 2.21) {0.08, 0.96}	1.84 (1.53, 2.24) {0.14, 0.80}	2.01 (1.78, 2.22) {0.07, 0.98}	1.64 (1.41, 1.89) {0.19, 0.44}
ϕ_y	0.5	0.23 (0.11, 0.40) {0.56, 0.32}	0.29 (0.14, 0.50) {0.49, 0.54}	0.13 (0.05, 0.22) {0.75, 0.02}	0.20 (0.05, 0.35) {0.65, 0.10}	0.24 (0.11, 0.41) {0.56, 0.30}	0.19 (0.08, 0.36) {0.64, 0.18}
Σ		3.86	4.80	5.02	6.96	3.91	4.81

Table 1: Average, $(5, 95)$ percentiles, and $\{\mathrm{NRMSE}, \mathrm{CR}\}$. Σ is the sum of the NRMSE across the parameters.

Lastly, we fixed φ_p and h to their true values and re-estimated each specification. Table 1 reports the results, which show how other parameters adjust. In particular, σ_s is now 3 to 4 times higher than its true value and ρ_s drops to roughly half of its true value. The NRMSEs for σ_s are by far the largest of any parameter and the CRs are all near 0. In this exercise, h cannot fall to compensate for the missing frictions, so the size of the risk premium shocks must increase. This effect, in addition to not allowing φ_p to increase to compensate for the lack of sticky wages, induces too much inflation volatility. Therefore, the estimate of risk premium persistence, ρ_s, falls. Unlike its shock size, its persistence affects the inflation response more than the output growth response.

Ptr	Truth	0Q	6Q	12Q	18Q	24Q	30Q
				NL-PF-5%			
φ_p	100	151.1 (134.2, 165.8) {0.52, 0.02}	161.0 (143.2, 179.3) {0.62, 0.00}	172.1 (153.8, 193.4) {0.73, 0.00}	180.6 (161.3, 201.4) {0.81, 0.18}	187.2 (167.0, 204.5) {0.88, 0.00}	188.4 (174.7, 202.7) {0.89, 0.00}
h	0.8	0.66 (0.62, 0.70) {0.18, 0.00}	0.66 (0.61, 0.71) {0.17, 0.00}	0.67 (0.62, 0.71) {0.17, 0.00}	0.67 (0.63, 0.71) {0.16, 0.00}	0.68 (0.64, 0.72) {0.15, 0.00}	0.68 (0.64, 0.71) {0.16, 0.00}
ρ_s	0.8	0.76 (0.72, 0.80) {0.06, 0.70}	0.77 (0.74, 0.81) {0.04, 0.86}	0.79 (0.75, 0.82) {0.03, 0.98}	0.80 (0.77, 0.84) {0.03, 0.92}	0.81 (0.78, 0.83) {0.02, 0.96}	0.81 (0.78, 0.84) {0.03, 0.90}
ρ_i	0.8	0.79 (0.75, 0.82) {0.03, 0.96}	0.79 (0.75, 0.82) {0.04, 0.90}	0.79 (0.77, 0.82) {0.02, 1.00}	0.80 (0.76, 0.83) {0.03, 0.94}	0.80 (0.76, 0.84) {0.03, 0.94}	0.80 (0.75, 0.84) {0.03, 0.96}
σ_z	0.0050	0.0032 (0.0023, 0.0039) {0.37, 0.00}	0.0032 (0.0023, 0.0041) {0.38, 0.08}	0.0034 (0.0024, 0.0044) {0.34, 0.18}	0.0037 (0.0027, 0.0049) {0.29, 0.38}	0.0038 (0.0027, 0.0047) {0.28, 0.46}	0.0040 (0.0030, 0.0052) {0.23, 0.58}
σ_s	0.0050	0.0052 (0.0040, 0.0066) {0.15, 0.92}	0.0052 (0.0042, 0.0068) {0.15, 0.92}	0.0051 (0.0040, 0.0060) {0.13, 0.98}	0.0051 (0.0034, 0.0064) {0.18, 0.86}	0.0050 (0.0041, 0.0064) {0.12, 1.00}	0.0050 (0.0039, 0.0062) {0.13, 0.96}
σ_i	0.0020	0.0017 (0.0014, 0.0020) {0.17, 0.48}	0.0017 (0.0014, 0.0019) {0.18, 0.40}	0.0016 (0.0014, 0.0019) {0.21, 0.30}	0.0016 (0.0013, 0.0019) {0.24, 0.26}	0.0015 (0.0013, 0.0018) {0.25, 0.20}	0.0015 (0.0013, 0.0019) {0.24, 0.20}
ϕ_π	2.0	2.04 (1.88, 2.19) {0.06, 0.98}	2.06 (1.87, 2.24) {0.07, 0.96}	2.12 (1.94, 2.33) {0.08, 0.92}	2.13 (1.90, 2.41) {0.10, 0.94}	2.10 (1.84, 2.33) {0.09, 0.90}	2.13 (1.94, 2.31) {0.09, 0.92}
ϕ_y	0.5	0.35 (0.21, 0.54) {0.36, 0.80}	0.39 (0.22, 0.61) {0.31, 0.92}	0.41 (0.27, 0.60) {0.27, 1.00}	0.40 (0.26, 0.54) {0.27, 0.92}	0.41 (0.26, 0.61) {0.27, 0.98}	0.42 (0.27, 0.62) {0.28, 0.98}
Σ		1.90	1.96	1.99	2.12	2.09	2.08
				OB-IF-0%			
φ_p	100	142.6 (121.1, 157.3) {0.44, 0.08}	152.5 (131.3, 170.7) {0.54, 0.02}	164.5 (140.8, 185.5) {0.66, 0.00}	174.7 (153.9, 202.0) {0.76, 0.00}	183.1 (165.3, 204.1) {0.84, 0.00}	183.4 (169.2, 198.5) {0.84, 0.00}
h	0.8	0.64 (0.61, 0.67) {0.20, 0.00}	0.64 (0.61, 0.68) {0.20, 0.00}	0.63 (0.60, 0.67) {0.21, 0.00}	0.63 (0.61, 0.67) {0.21, 0.00}	0.63 (0.59, 0.67) {0.21, 0.00}	0.63 (0.60, 0.67) {0.21, 0.00}
ρ_s	0.8	0.76 (0.73, 0.81) {0.05, 0.82}	0.77 (0.73, 0.81) {0.04, 0.92}	0.80 (0.76, 0.83) {0.03, 0.96}	0.81 (0.78, 0.85) {0.03, 0.86}	0.82 (0.80, 0.85) {0.03, 0.76}	0.82 (0.79, 0.86) {0.04, 0.78}
ρ_i	0.8	0.76 (0.71, 0.79) {0.06, 0.52}	0.75 (0.71, 0.80) {0.07, 0.50}	0.76 (0.73, 0.79) {0.06, 0.54}	0.76 (0.68, 0.80) {0.06, 0.58}	0.76 (0.72, 0.81) {0.06, 0.58}	0.77 (0.73, 0.81) {0.05, 0.66}
σ_z	0.0050	0.0051 (0.0044, 0.0058) {0.09, 0.92}	0.0053 (0.0048, 0.0068) {0.13, 0.82}	0.0056 (0.0047, 0.0066) {0.19, 0.60}	0.0059 (0.0051, 0.0079) {0.24, 0.54}	0.0060 (0.0051, 0.0074) {0.25, 0.46}	0.0059 (0.0050, 0.0069) {0.22, 0.30}
σ_s	0.0050	0.0051 (0.0042, 0.0063) {0.13, 0.92}	0.0051 (0.0041, 0.0063) {0.14, 0.96}	0.0048 (0.0039, 0.0058) {0.13, 0.90}	0.0047 (0.0031, 0.0058) {0.18, 0.76}	0.0045 (0.0037, 0.0053) {0.15, 0.80}	0.0046 (0.0036, 0.0056) {0.15, 0.82}
σ_i	0.0020	0.0020 (0.0018, 0.0023) {0.08, 0.90}	0.0020 (0.0018, 0.0023) {0.07, 0.90}	0.0020 (0.0018, 0.0022) {0.07, 0.98}	0.0020 (0.0018, 0.0024) {0.09, 0.82}	0.0020 (0.0018, 0.0023) {0.08, 0.88}	0.0020 (0.0019, 0.0024) {0.09, 0.90}
ϕ_π	2.0	2.01 (1.84, 2.16) {0.06, 0.98}	1.96 (1.77, 2.16) {0.07, 0.98}	1.99 (1.78, 2.16) {0.06, 0.98}	1.97 (1.73, 2.23) {0.08, 0.96}	1.94 (1.69, 2.19) {0.08, 0.90}	1.96 (1.77, 2.14) {0.06, 0.98}
ϕ_y	0.5	0.32 (0.17, 0.48) {0.41, 0.68}	0.35 (0.18, 0.53) {0.37, 0.76}	0.39 (0.24, 0.56) {0.30, 0.90}	0.36 (0.20, 0.52) {0.35, 0.80}	0.41 (0.21, 0.62) {0.29, 0.90}	0.44 (0.27, 0.61) {0.25, 0.98}
Σ		1.53	1.63	1.71	2.01	1.99	1.91

Table 2: Average, $(5, 95)$ percentiles, and $\{\text{NRMSE}, \text{CR}\}$. Σ is the sum of the NRMSE across the parameters.

Ptr	Truth	0Q	6Q	12Q	18Q	24Q	30Q
				Lin-KF-0%			
φ_p	100	143.0	153.3	167.2	177.5	186.3	186.9
		(125.9, 157.7)	(134.2, 168.4)	(147.0, 196.6)	(157.1, 204.9)	(165.6, 204.5)	(168.5, 201.1)
		{0.44, 0.04}	{0.54, 0.00}	{0.69, 0.00}	{0.79, 0.00}	{0.87, 0.00}	{0.88, 0.00}
h	0.8	0.64	0.64	0.64	0.64	0.64	0.63
		(0.61, 0.68)	(0.60, 0.68)	(0.60, 0.67)	(0.62, 0.67)	(0.60, 0.67)	(0.60, 0.67)
		{0.20, 0.00}	{0.20, 0.00}	{0.20, 0.00}	{0.20, 0.00}	{0.20, 0.00}	{0.21, 0.00}
ρ_s	0.8	0.76	0.77	0.80	0.81	0.82	0.82
		(0.72, 0.80)	(0.74, 0.80)	(0.76, 0.83)	(0.76, 0.84)	(0.80, 0.85)	(0.80, 0.85)
		{0.06, 0.74}	{0.04, 0.88}	{0.03, 1.00}	{0.03, 0.92}	{0.03, 0.82}	{0.04, 0.78}
ρ_i	0.8	0.76	0.77	0.78	0.79	0.80	0.81
		(0.73, 0.79)	(0.72, 0.80)	(0.75, 0.81)	(0.74, 0.84)	(0.77, 0.85)	(0.77, 0.85)
		{0.06, 0.62}	{0.05, 0.70}	{0.04, 0.92}	{0.03, 0.88}	{0.03, 0.90}	{0.03, 0.90}
σ_z	0.0050	0.0049	0.0051	0.0055	0.0057	0.0060	0.0059
		(0.0043, 0.0054)	(0.0045, 0.0058)	(0.0048, 0.0066)	(0.0051, 0.0067)	(0.0049, 0.0071)	(0.0051, 0.0068)
		{0.07, 0.90}	{0.08, 0.88}	{0.16, 0.56}	{0.17, 0.50}	{0.23, 0.32}	{0.21, 0.28}
σ_s	0.0050	0.0052	0.0051	0.0048	0.0048	0.0045	0.0045
		(0.0043, 0.0064)	(0.0042, 0.0062)	(0.0040, 0.0058)	(0.0035, 0.0059)	(0.0038, 0.0053)	(0.0036, 0.0052)
		{0.14, 0.86}	{0.14, 0.96}	{0.12, 0.96}	{0.15, 0.86}	{0.15, 0.78}	{0.15, 0.86}
σ_i	0.0020	0.0020	0.0020	0.0020	0.0020	0.0020	0.0019
		(0.0018, 0.0022)	(0.0018, 0.0022)	(0.0018, 0.0023)	(0.0016, 0.0022)	(0.0017, 0.0022)	(0.0017, 0.0022)
		{0.07, 0.96}	{0.07, 0.88}	{0.08, 0.88}	{0.08, 0.82}	{0.08, 0.88}	{0.08, 0.88}
ϕ_π	2.0	2.01	1.96	1.85	1.78	1.65	1.69
		(1.85, 2.15)	(1.71, 2.17)	(1.60, 2.07)	(1.51, 2.04)	(1.42, 1.92)	(1.46, 1.89)
		{0.06, 0.98}	{0.07, 1.00}	{0.10, 0.94}	{0.14, 0.76}	{0.19, 0.44}	{0.17, 0.64}
ϕ_y	0.5	0.32	0.32	0.28	0.26	0.25	0.28
		(0.18, 0.48)	(0.20, 0.52)	(0.11, 0.48)	(0.14, 0.43)	(0.15, 0.37)	(0.17, 0.44)
		{0.40, 0.72}	{0.41, 0.60}	{0.48, 0.50}	{0.51, 0.32}	{0.51, 0.32}	{0.47, 0.44}
Σ		1.49	1.62	1.89	2.10	2.30	2.24
				Lin-KF-5%			
φ_p	100	151.4	161.1	174.8	183.1	191.1	191.6
		(134.0, 165.7)	(142.0, 179.5)	(153.7, 198.6)	(163.0, 208.5)	(172.1, 210.9)	(175.3, 204.1)
		{0.52, 0.00}	{0.62, 0.00}	{0.76, 0.00}	{0.84, 0.00}	{0.92, 0.00}	{0.92, 0.00}
h	0.8	0.66	0.66	0.67	0.67	0.67	0.67
		(0.62, 0.69)	(0.61, 0.71)	(0.62, 0.71)	(0.63, 0.70)	(0.64, 0.71)	(0.63, 0.70)
		{0.18, 0.00}	{0.18, 0.00}	{0.17, 0.00}	{0.17, 0.00}	{0.16, 0.00}	{0.17, 0.00}
ρ_s	0.8	0.76	0.78	0.80	0.81	0.82	0.82
		(0.72, 0.80)	(0.74, 0.81)	(0.75, 0.83)	(0.78, 0.85)	(0.79, 0.85)	(0.78, 0.86)
		{0.06, 0.74}	{0.04, 0.92}	{0.03, 1.00}	{0.03, 0.00}	{0.03, 0.88}	{0.04, 0.78}
ρ_i	0.8	0.79	0.80	0.81	0.83	0.83	0.84
		(0.75, 0.82)	(0.75, 0.83)	(0.78, 0.84)	(0.78, 0.86)	(0.80, 0.88)	(0.80, 0.88)
		{0.03, 0.98}	{0.04, 0.96}	{0.03, 0.94}	{0.04, 0.00}	{0.05, 0.70}	{0.06, 0.56}
σ_z	0.0050	0.0032	0.0033	0.0036	0.0040	0.0042	0.0043
		(0.0023, 0.0039)	(0.0025, 0.0041)	(0.0027, 0.0045)	(0.0029, 0.0052)	(0.0029, 0.0054)	(0.0030, 0.0057)
		{0.36, 0.00}	{0.36, 0.12}	{0.31, 0.32}	{0.24, 0.00}	{0.22, 0.66}	{0.20, 0.68}
σ_s	0.0050	0.0053	0.0052	0.0051	0.0050	0.0048	0.0047
		(0.0040, 0.0067)	(0.0042, 0.0068)	(0.0041, 0.0062)	(0.0033, 0.0063)	(0.0039, 0.0059)	(0.0037, 0.0061)
		{0.15, 0.92}	{0.15, 0.90}	{0.14, 0.94}	{0.18, 0.00}	{0.12, 0.96}	{0.15, 0.92}
σ_i	0.0020	0.0017	0.0016	0.0017	0.0016	0.0016	0.0016
		(0.0015, 0.0020)	(0.0014, 0.0019)	(0.0014, 0.0020)	(0.0012, 0.0019)	(0.0014, 0.0020)	(0.0014, 0.0019)
		{0.16, 0.50}	{0.20, 0.20}	{0.17, 0.44}	{0.22, 0.00}	{0.19, 0.32}	{0.20, 0.28}
ϕ_π	2.0	2.04	2.00	1.89	1.83	1.72	1.73
		(1.88, 2.20)	(1.72, 2.21)	(1.67, 2.09)	(1.62, 2.09)	(1.52, 1.93)	(1.52, 1.91)
		{0.06, 0.98}	{0.07, 1.00}	{0.08, 1.00}	{0.11, 0.00}	{0.16, 0.78}	{0.15, 0.78}
ϕ_y	0.5	0.35	0.36	0.33	0.31	0.31	0.32
		(0.22, 0.54)	(0.21, 0.56)	(0.14, 0.54)	(0.18, 0.50)	(0.19, 0.45)	(0.17, 0.47)
		{0.35, 0.80}	{0.36, 0.84}	{0.42, 0.70}	{0.43, 0.00}	{0.42, 0.66}	{0.40, 0.76}
Σ		1.88	2.01	2.11	2.27	2.28	2.28

Table 3: Average, (5, 95) percentiles, and {NRMSE, CR}. Σ is the sum of the NRMSE across the parameters.

9

E.2 SHORTER ZLB DURATIONS   The paper focuses on the accuracy of NL-PF and OB-IF in datasets with either no ZLB events or a single 30 quarter event. This section shows the results when the ZLB binds for durations that are shorter than 30 quarters. We show the NRMSE for each estimated parameter as well as the sum of the NRMSE to measure overall accuracy. Table 2 shows the results with NL-PF-5% and OB-IF-0%, while table 3 focuses on Lin-KF-0% and Lin-KF-5%.

| Ptr | Truth | No Misspecification: DGP and Estimation Use Small-Scale Model | | | | | |
| | | NL-PF-5% | | OB-IF-0% | | Lin-KF-5% | |
		0Q	30Q	0Q	30Q	0Q	30Q
φ_p	100	96.8 (81.6, 109.9) {0.09, 0.96}	109.8 (89.5, 130.3) {0.15, 0.90}	94.3 (81.8, 108.3) {0.11, 0.96}	110.6 (95.3, 125.1) {0.15, 0.96}	103.7 (92.6, 118.4) {0.09, 0.98}	128.5 (111.2, 145.3) {0.30, 0.46}
h	0.8	0.79 (0.76, 0.82) {0.02, 0.94}	0.79 (0.77, 0.82) {0.02, 0.94}	0.79 (0.75, 0.82) {0.02, 0.92}	0.79 (0.77, 0.82) {0.02, 0.96}	0.80 (0.76, 0.83) {0.02, 0.96}	0.79 (0.76, 0.82) {0.03, 0.92}
ρ_s	0.8	0.80 (0.76, 0.83) {0.03, 0.96}	0.83 (0.78, 0.86) {0.04, 0.60}	0.81 (0.76, 0.85) {0.04, 0.98}	0.84 (0.80, 0.87) {0.06, 0.58}	0.82 (0.77, 0.86) {0.05, 0.90}	0.87 (0.83, 0.91) {0.10, 0.10}
ρ_i	0.8	0.82 (0.79, 0.84) {0.03, 0.88}	0.82 (0.78, 0.85) {0.03, 0.80}	0.79 (0.77, 0.82) {0.02, 0.98}	0.79 (0.74, 0.82) {0.03, 0.90}	0.82 (0.79, 0.84) {0.03, 0.94}	0.86 (0.83, 0.88) {0.08, 0.26}
σ_z	0.005	0.0037 (0.0029, 0.0046) {0.27, 0.24}	0.0035 (0.0025, 0.0045) {0.33, 0.18}	0.0051 (0.0044, 0.0056) {0.08, 0.98}	0.0052 (0.0043, 0.0061) {0.11, 0.86}	0.0038 (0.0029, 0.0046) {0.26, 0.28}	0.0034 (0.0026, 0.0044) {0.33, 0.16}
σ_s	0.005	0.0047 (0.0035, 0.0058) {0.19, 0.90}	0.0043 (0.0032, 0.0058) {0.22, 0.72}	0.0049 (0.0039, 0.0060) {0.16, 0.86}	0.0046 (0.0034, 0.0057) {0.17, 0.80}	0.0047 (0.0034, 0.0059) {0.21, 0.90}	0.0036 (0.0027, 0.0046) {0.32, 0.38}
σ_i	0.002	0.0016 (0.0013, 0.0020) {0.20, 0.24}	0.0014 (0.0010, 0.0018) {0.31, 0.18}	0.0020 (0.0017, 0.0022) {0.07, 0.90}	0.0019 (0.0016, 0.0022) {0.10, 0.78}	0.0016 (0.0013, 0.0019) {0.20, 0.24}	0.0015 (0.0012, 0.0017) {0.27, 0.10}
ϕ_π	2.0	2.00 (1.81, 2.21) {0.06, 0.96}	2.01 (1.82, 2.20) {0.06, 1.00}	1.95 (1.74, 2.14) {0.06, 1.00}	1.80 (1.58, 2.06) {0.12, 0.76}	1.97 (1.76, 2.18) {0.07, 0.96}	1.62 (1.42, 1.86) {0.20, 0.38}
ϕ_y	0.5	0.45 (0.29, 0.61) {0.22, 1.00}	0.48 (0.28, 0.61) {0.18, 1.00}	0.46 (0.30, 0.63) {0.21, 1.00}	0.52 (0.32, 0.73) {0.23, 1.00}	0.46 (0.31, 0.63) {0.22, 1.00}	0.50 (0.34, 0.66) {0.19, 1.00}
Σ		1.12	1.35	0.78	0.99	1.14	1.82

Table 4: Average, $(5, 95)$ percentiles, and $\{\text{NRMSE}, \text{CR}\}$. Σ is the sum of the NRMSE across the parameters.

E.3 NO MISSPECIFICATION   Table 4 compares the parameter estimates after removing model misspecification. Since it is numerically very expensive to estimate the medium-scale model used to generate the data with NL-PF, we created new datasets from the small-scale model. The sum of the NRMSE shows about 40% of the error is due to model misspecification. For example, in datasets without any ZLB events, the error with NL-PF-5% increases from 1.12 to 1.90 when misspecification is added to the estimated model. Removing misspecification has the largest impact on the accuracy of φ_p, h, and ϕ_y because the estimates no longer have to compensate for the lack of sticky wages and investment, which creates large differences in the model's sensitivity to shocks. Notably, the NL-PF-5% estimate of φ_p declines from 151.1 to 96.8 and the estimate of h rises from 0.66 to 0.79 in datasets without ZLB events. The CR rises from near 0 to consistently above 0.9.

The other results emphasized in the paper are unchanged. The shock standard deviations are biased downward with NL-PF-5% because the filter incorrectly assigns some of the fluctuations to ME, reducing the estimated variances. When the ZLB binds in the data, it biases the estimates of φ_p and ρ_s upward, though NL-PF-5% and OB-IF-0% are both far more accurate than Lin-KF-5%.
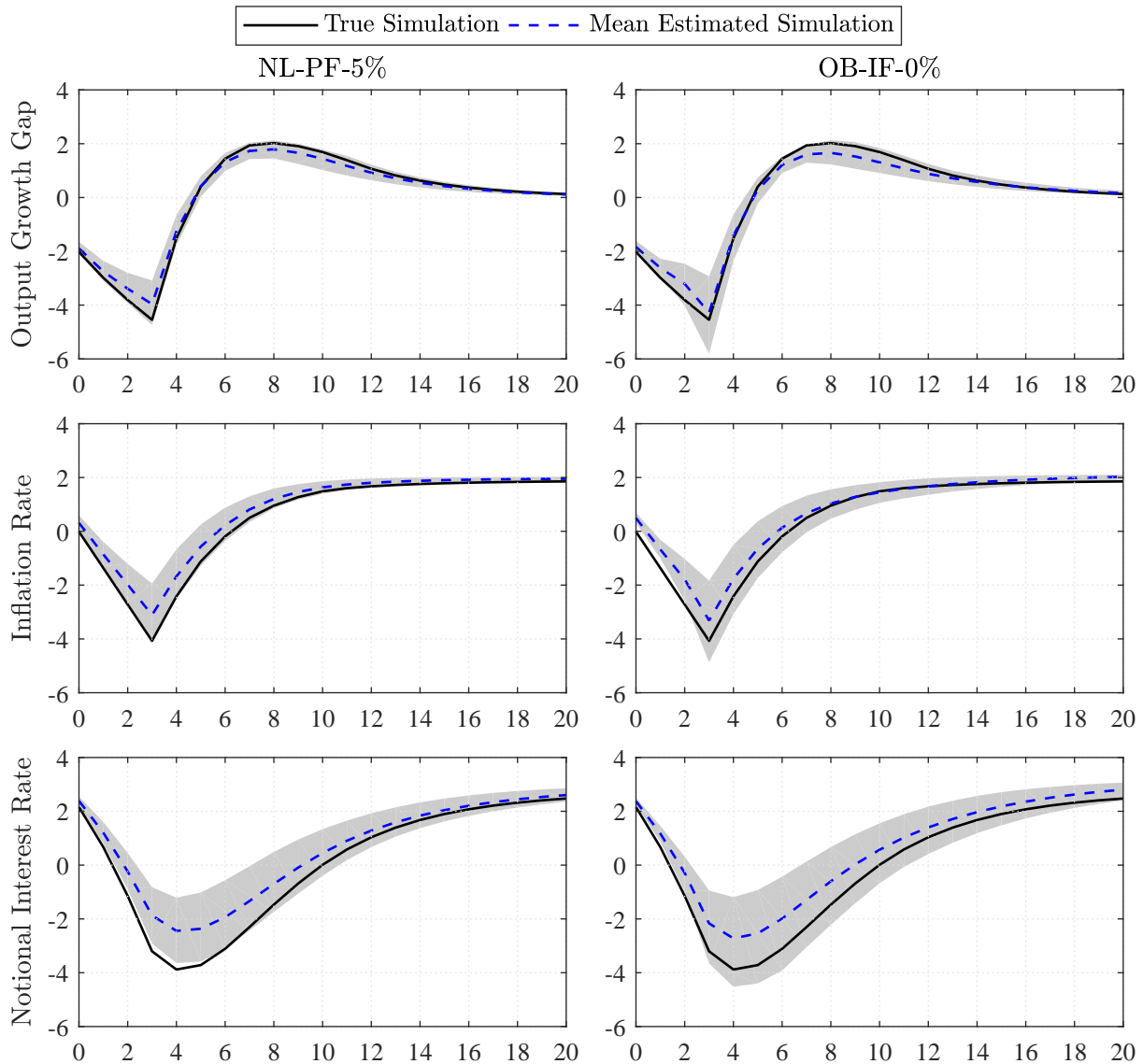

Figure 2: Recession responses without model misspecification. The solid line is the true simulation, the dashed line is the mean estimated simulation, and the shaded area contains the $(5, 95)$ percentiles across the datasets. The simulations are initialized in steady state and followed by four consecutive 1.5 standard deviation positive risk premium shocks.

Figure 2 plots the recession responses in figure 3 without misspecification. The solid line shows the responses based on the true parameterization of the small-scale model, rather than the medium-scale model that generates our original datasets. The dashed line shows the mean responses, given the parameter estimates with our alternative datasets. Consistent with the previous results, the responses based on the NL-PF-5% and OB-IF-0% parameter estimates are very similar. The key dif-

ference is that the mean estimated simulations are much closer to the true simulation and the $(5, 95)$ percentiles almost always encompass the truth. This result shows the muted responses in figure 3 are primarily driven by model misspecification, rather than inaccuracies in the estimation methods.

E.4 IMPULSE RESPONSES   This section shows generalized impulse response functions (GIRFs) of a productivity growth and monetary policy shock when the economy is in a severe recession and the ZLB binds. To compute the GIRFs, we follow Koop et al. (1996). We first calculate the mean of 10,000 simulations, conditional on random shocks in every quarter (i.e., the baseline path). We then calculate a second mean from another set of 10,000 simulations, but this time the shock in the first quarter is replaced with a two standard deviation negative productivity growth or monetary policy shock (i.e., the impulse path). Finally, we plot the differences between the two mean paths.

The benefit of a GIRF over a more traditional impulse response function is that it allows us to calculate the responses in any state of the economy without the influence of mean reversion. For the true model, we initialize at the state following four consecutive 1.5 standard deviation positive risk premium shocks, consistent with figure 3. We then find a sequence of four equally sized risk premium shocks that produce the same notional rate in our estimated model as the true model, so the simulations begin at the same point. The NL-PF-5% simulations are shown in the left column and the OB-IF-0% simulations are in the right column. The true simulation of the DGP (solid line) is compared to the mean estimated simulation of the small-scale model (dashed line). The $(5, 95)$ percentiles account for differences in the simulations across the parameter estimates for each dataset.

Figure 3a shows the responses to a productivity growth shock. Qualitatively the responses of output growth and inflation are similar across the specifications. Higher productivity growth increases the output growth gap and decreases the inflation rate like a typical supply shock. Since the Fed faces a tradeoff between stabilizing the inflation and output gaps, the notional interest rate response depends on the parameterization. The notional rate rises with the DGP, but falls with both of the estimated models. Quantitatively, there are important differences between all of the responses. Consistent with figure 3, model misspecification leads to muted responses of the output growth gap and the inflation rate. There are also differences in the magnitudes of the estimated responses, but most of that is driven by the downward bias in the shock standard deviation with NL-PF-5%.

Figure 3b shows the responses to a monetary policy shock. Although the ZLB binds in the true and estimated models, the shock is expansionary because it lowers the expected nominal interest rate in future periods. Therefore, the output growth gap and the inflation rate both increase in all three models. Unlike with the other two shocks, model misspecification has a relatively small effect on the responses, as the $(5, 95)$ percentiles of the estimated responses encompass the true responses in most periods. There are some differences in the NL-PF-5% and OB-IF-0% responses, but they are smaller than in figure 3a and are never large enough to have meaningful policy implications.

(a) Productivity Growth Shock
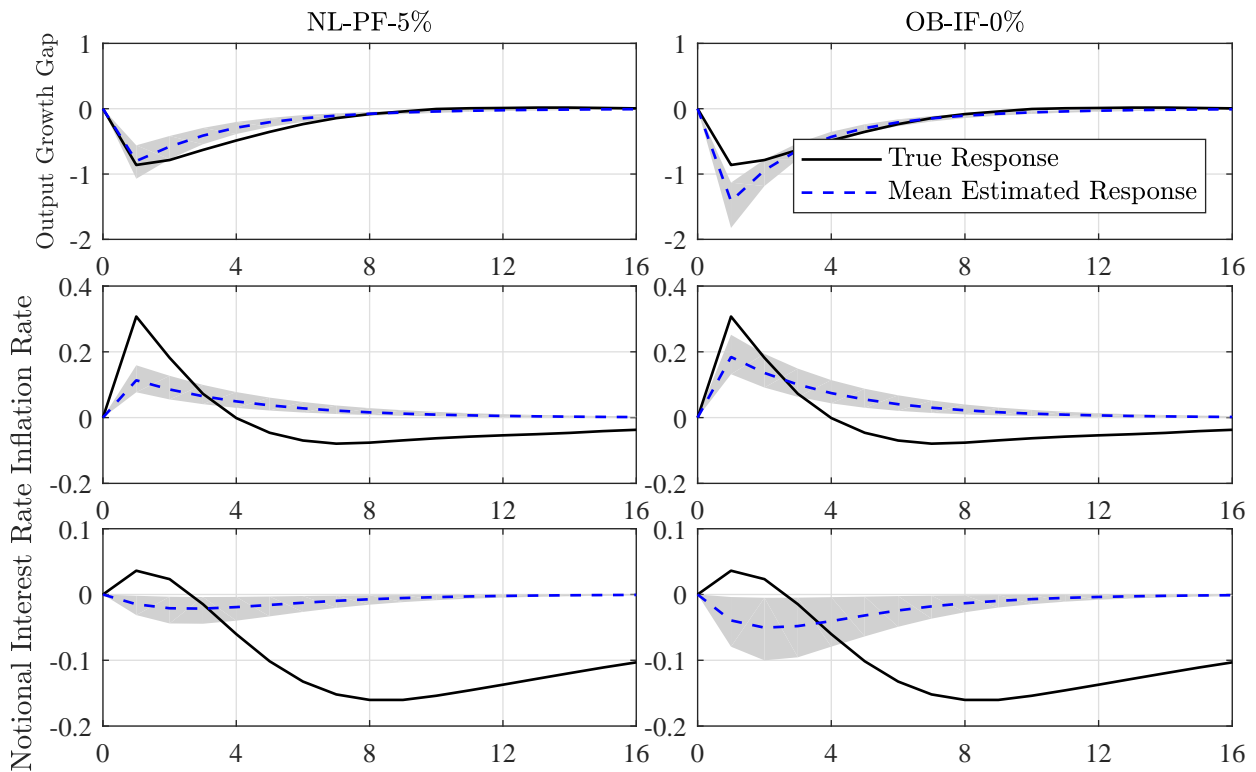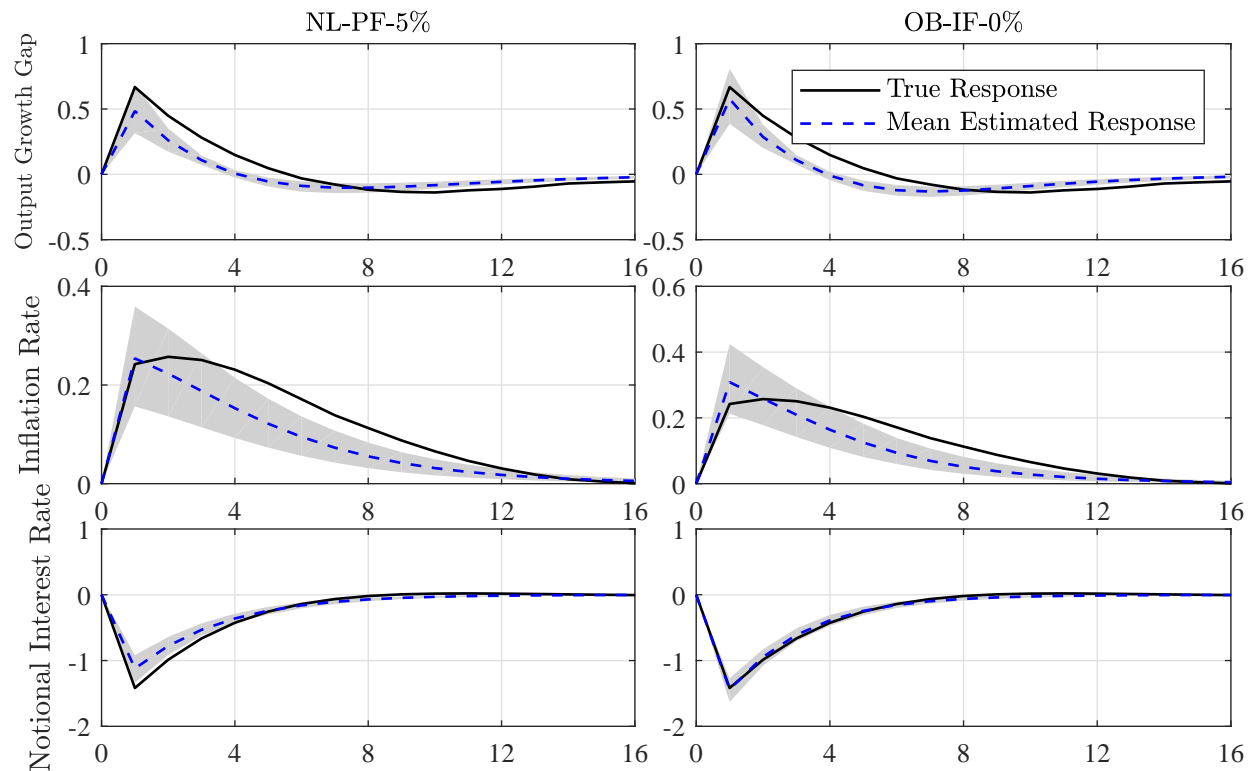

(b) Monetary Policy Shock

Figure 3: Impulse responses to a -2 standard deviation shock in a severe recession. The solid line is the true response, the dashed line is the mean estimated response, and the shaded area contains the $(5, 95)$ percentiles of the responses.
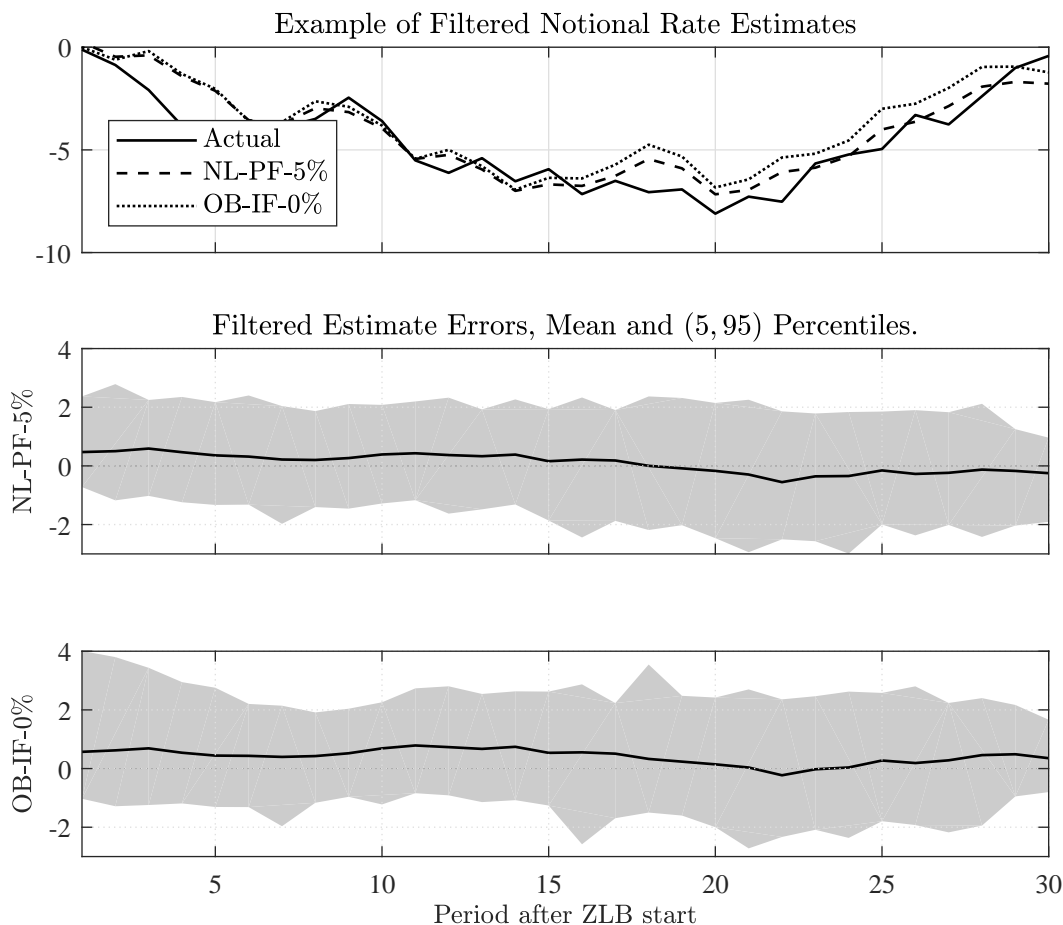
Figure 4: Estimates of the notional rate in datasets with a 30 quarter ZLB event. Rates are net annualized percentages.

E.5 NOTIONAL RATE ESTIMATES   Figure 4 provides more intuition about what is driving the relative accuracy of the filtered estimates of the notional rate in figure 1. The top panel plots the actual notional rate from an example dataset with a 30 quarter ZLB event, as well as the filtered estimates from NL-PF-5% and OB-IF-0%. Over time, the OB-IF-0% estimate increases towards zero faster than NL-PF-5%. This may be driven by the lower estimate of ρ_i (0.77) with OB-IF-0%, which is slightly below the NL-PF-5% estimate and the true value (0.80). The bottom two panels plot the error in the average filtered notional rate estimates during the 30 quarter ZLB event across the 50 datasets (solid line). The shaded region shows the (5, 95) percentiles. This suggests the example dataset in the top panel is fairly representative. The distribution of errors for OB-IF-0% is slightly shifted up from the NL-PF-5% error distribution, and increasingly so over time. This may seem somewhat at odds with the results in figure 1, as OB-IF-0% is even less accurate relative to NL-PF-5% in the datasets with shorter ZLB events. However the OB-IF-0% estimates of ρ_i and ϕ_y have an even larger downward bias in datasets with shorter ZLB duration, as shown in table 2.

E.6 ADDITIONAL DATASET STATISTICS   ZLB events are frequent in the medium-scale model that generates the datasets, which allows us to find simulations with up to 30 consecutive quarters

	6Q	12Q	18Q	24Q	30Q
CDF of ZLB Event Durations	0.678	0.885	0.966	0.992	0.998
Number of Simulations to Reach 50 Datasets	150,300	154,950	256,950	391,950	1,030,300

Table 5: Probability of ZLB event durations in a long simulation of the medium-scale model.
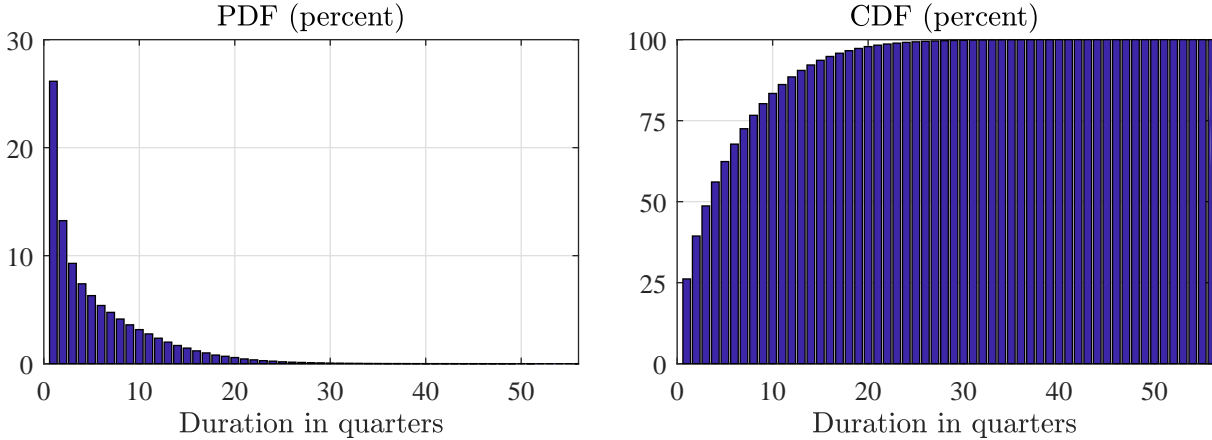

Figure 5: Duration of ZLB events in a long simulation of the medium-scale model.

at the ZLB without imposing restrictions on the shocks. In a long simulation of the model, the unconditional probability of being at the ZLB is 24 percent. This is roughly equivalent to the U.S. experience of 7 years, since our sample is 30 years. Most of the ZLB events in the simulation are short, with the policy rate rising above zero within one year or less, as shown in table 5 and figure 5. However, long ZLB events are not incredibly uncommon, as 0.25 percent of ZLB events have a duration of at least 30 quarters. When generating our datasets, we impose an additional requirement that the ZLB event in our sample is unique so it reflects actual data. The number of 120 quarter simulations required to find 50 simulations that meet that criterion is shown in the last row of table 5.

E.7 GOVERNMENT SPENDING   This section shows how government spending affects our results. Government spending is a potentially important feature because it adds a shock that directly enters the aggregate resource constraint. Without government spending, any shock in the DGP that affects the resource constraint is absorbed by consumption or price adjustment costs in the small-scale model, since output and inflation are observed. Without a wedge between consumption and output, it could cause significant bias in the habit persistence and price adjustment cost parameters.

We assume the share of government spending devoted to output follows

$$g_t^s = (1 - \rho_g)\bar{g}^s + \rho_g g_{t-1}^s + \sigma_g \varepsilon_{g,t}, 0 \leq \rho_g < 1, \varepsilon_g \sim \mathbb{N}(0,1), \tag{22}$$

where the steady-state share, $\bar{g}^s$, is set to 0.2129 to match the time average from 1988Q1-2017Q4.

15

With the addition of government spending, the aggregate resource constraint is given by

$$c_t + x_t = (1 - g_t^s)y_t^{gdp}. \tag{23}$$

All other equations in the equilibrium system are unchanged. We add government spending to the medium-scale model that generates our datasets and our small-scale model for estimation. We estimate the small-scale model with (g^s-4obs) and without (g^s-3obs) including real per capita consumption growth as an additional observable. In this second specification, the government spending shock is less constrained, potentially absorbing the adjustment costs left out of the small-scale model and reducing inaccuracy driven by misspecification in the aggregate resource constraint. The specification without government spending (no-g^s) excludes g^s from the DGP and the estimated model, just like in the main paper. In each case, the true parameterization is unchanged, except the shock standard deviations were reduced from 0.005 to 0.004. This change is necessary because the additional volatility in the model with government spending causes the model to spend too much time at the ZLB and not converge at the previous parameterization. Table 6 shows the parameter estimates using datasets where the ZLB binds for 30 quarters and table 7 is based on datasets where the ZLB never binds in the data. OB-IF-0% is not used to estimate these specifications, since it is not possible to have more shocks than observables in the inversion filter.

Interestingly, the differences in the parameter estimates between g^s-4obs and no-g^s are fairly small, especially in datasets where the ZLB binds for 30 quarters. The g^s-4obs estimates of φ_p and h are more accurate than the no-g^s estimates, but they are still significantly biased. Furthermore, the improvement in those estimates is not as significant as what occurs when we add sticky wages to the model estimated with OB-IF-0%. This implies that the presence of government spending helps increase the volatility of output growth, but not enough to compensate for the lack of sticky wages, which we see as the most important misspecification driving the bias in φ_p and h. It is also important to note that the estimates of the productivity growth and risk premium shock standard deviations (σ_z and σ_s) are biased downward to a greater extent than in the model without government spending. As a consequence, the sum of the NRMSE with government spending is higher than without government spending, regardless of the estimation method or the duration of the ZLB. This result occurs even though the g^s-4obs estimates included an additional observable.

Excluding the additional observable (g^s-3obs) also does not improve the overall accuracy of the parameter estimates. The productivity growth and risk premium shock standard deviations become more accurate than no-g^s, but the estimates of φ_p are largely unchanged and the downward bias in h becomes even larger. As a result, the NRMSE of g^s-3obs is higher than the g^s-4obs or no-g^s estimates. Once again, this is consistent with the lack of sticky wages as the most important misspecification, while misspecification in the resource constraint appears to play a smaller role.

Ptr	Truth	NL-PF-5% (30Q)			Lin-KF-5% (30Q)		
		no-g^s	g^s-4obs	g^s-3obs	no-g^s	g^s-4obs	g^s-3obs
φ_p	100	180.8 (167.2, 193.5) {0.81, 0.00}	164.2 (145.1, 188.9) {0.65, 0.06}	183.3 (165.2, 203.5) {0.84, 0.00}	182.8 (168.0, 194.5) {0.83, 0.00}	170.0 (150.3, 196.3) {0.71, 0.00}	188.6 (167.6, 210.5) {0.90, 0.00}
h	0.8	0.66 (0.63, 0.71) {0.17, 0.00}	0.71 (0.67, 0.74) {0.11, 0.00}	0.56 (0.47, 0.62) {0.31, 0.00}	0.65 (0.62, 0.70) {0.18, 0.00}	0.71 (0.66, 0.74) {0.12, 0.00}	0.54 (0.43, 0.61) {0.33, 0.00}
ρ_s	0.8	0.84 (0.81, 0.86) {0.05, 0.48}	0.86 (0.84, 0.88) {0.08, 0.10}	0.84 (0.80, 0.87) {0.05, 0.62}	0.85 (0.82, 0.87) {0.06, 0.36}	0.87 (0.85, 0.90) {0.09, 0.12}	0.84 (0.81, 0.88) {0.06, 0.58}
ρ_i	0.8	0.81 (0.78, 0.84) {0.03, 0.94}	0.81 (0.77, 0.84) {0.03, 0.96}	0.81 (0.77, 0.85) {0.03, 0.92}	0.83 (0.80, 0.86) {0.04, 0.80}	0.83 (0.80, 0.88) {0.05, 0.70}	0.85 (0.81, 0.89) {0.07, 0.28}
ρ_{gs}	0.8	–	0.89 (0.85, 0.93) {0.12, 0.28}	0.82 (0.80, 0.84) {0.03, 1.00}	–	0.89 (0.85, 0.93) {0.12, 0.20}	0.83 (0.82, 0.86) {0.04, 1.00}
σ_z	0.004	0.0030 (0.0023, 0.0037) {0.26, 0.40}	0.0028 (0.0019, 0.0037) {0.33, 0.20}	0.0034 (0.0026, 0.0047) {0.21, 0.94}	0.0031 (0.0024, 0.0038) {0.25, 0.40}	0.0029 (0.0021, 0.0041) {0.30, 0.28}	0.0036 (0.0025, 0.0052) {0.22, 0.88}
σ_s	0.004	0.0031 (0.0025, 0.0039) {0.25, 0.50}	0.0024 (0.0020, 0.0030) {0.40, 0.04}	0.0036 (0.0026, 0.0049) {0.20, 0.82}	0.0029 (0.0023, 0.0036) {0.30, 0.26}	0.0023 (0.0018, 0.0029) {0.44, 0.00}	0.0034 (0.0025, 0.0047) {0.22, 0.70}
σ_i	0.002	0.0015 (0.0013, 0.0018) {0.24, 0.22}	0.0015 (0.0011, 0.0018) {0.26, 0.28}	0.0015 (0.0011, 0.0017) {0.29, 0.22}	0.0014 (0.0011, 0.0016) {0.33, 0.00}	0.0015 (0.0012, 0.0017) {0.26, 0.10}	0.0015 (0.0012, 0.0017) {0.27, 0.10}
σ_g	0.004	–	0.0044 (0.0039, 0.0049) {0.13, 0.74}	0.0025 (0.0018, 0.0032) {0.39, 0.16}	–	0.0044 (0.0039, 0.0049) {0.13, 0.70}	0.0025 (0.0018, 0.0033) {0.40, 0.20}
ϕ_π	2.0	2.27 (2.13, 2.47) {0.14, 0.64}	2.09 (1.85, 2.34) {0.08, 0.90}	2.23 (2.00, 2.45) {0.13, 0.68}	2.10 (1.91, 2.32) {0.08, 0.92}	1.73 (1.31, 2.04) {0.17, 0.72}	1.90 (1.62, 2.13) {0.09, 0.96}
ϕ_y	0.5	0.38 (0.26, 0.55) {0.29, 0.98}	0.50 (0.34, 0.63) {0.18, 0.98}	0.47 (0.24, 0.64) {0.21, 0.96}	0.36 (0.22, 0.51) {0.33, 0.94}	0.41 (0.30, 0.58) {0.25, 0.98}	0.44 (0.31, 0.64) {0.23, 0.98}
Σ		2.26	2.38	2.70	2.39	2.64	2.83

Table 6: Average, $(5, 95)$ percentiles, and $\{\text{NRMSE}, \text{CR}\}$. Σ is the sum of the NRMSE across the parameters.

Ptr	Truth	NL-PF-5% (0Q)			Lin-KF-5% (0Q)		
		no-g^s	g^s-4obs	g^s-3obs	no-g^s	g^s-4obs	g^s-3obs
φ_p	100	157.9 (130.0, 175.8) {0.59, 0.00}	128.8 (109.2, 143.7) {0.31, 0.34}	148.8 (128.8, 163.8) {0.50, 0.00}	157.7 (130.1, 175.3) {0.59, 0.02}	128.8 (109.5, 142.8) {0.31, 0.38}	149.2 (129.4, 164.3) {0.50, 0.00}
h	0.8	0.64 (0.60, 0.69) {0.20, 0.00}	0.68 (0.65, 0.72) {0.15, 0.00}	0.57 (0.47, 0.66) {0.30, 0.00}	0.64 (0.60, 0.69) {0.20, 0.00}	0.68 (0.65, 0.72) {0.15, 0.00}	0.57 (0.48, 0.66) {0.29, 0.00}
ρ_s	0.8	0.79 (0.74, 0.82) {0.03, 0.94}	0.81 (0.76, 0.85) {0.03, 0.90}	0.78 (0.72, 0.83) {0.05, 0.86}	0.79 (0.74, 0.83) {0.03, 0.96}	0.81 (0.77, 0.85) {0.04, 0.90}	0.78 (0.72, 0.83) {0.05, 0.86}
ρ_i	0.8	0.79 (0.74, 0.82) {0.04, 0.86}	0.78 (0.74, 0.82) {0.04, 0.84}	0.80 (0.76, 0.83) {0.03, 0.98}	0.79 (0.74, 0.82) {0.04, 0.88}	0.78 (0.75, 0.82) {0.03, 0.92}	0.80 (0.76, 0.83) {0.03, 0.98}
ρ_{gs}	0.8	—	0.82 (0.76, 0.87) {0.05, 0.94}	0.81 (0.76, 0.84) {0.03, 1.00}	—	0.82 (0.77, 0.86) {0.04, 0.94}	0.80 (0.75, 0.83) {0.03, 1.00}
σ_z	0.004	0.0029 (0.0022, 0.0037) {0.29, 0.22}	0.0023 (0.0018, 0.0029) {0.43, 0.00}	0.0027 (0.0019, 0.0036) {0.36, 0.54}	0.0029 (0.0022, 0.0037) {0.29, 0.28}	0.0023 (0.0018, 0.0029) {0.43, 0.00}	0.0027 (0.0019, 0.0036) {0.36, 0.50}
σ_s	0.004	0.0032 (0.0025, 0.0038) {0.23, 0.52}	0.0025 (0.0021, 0.0030) {0.38, 0.02}	0.0036 (0.0026, 0.0049) {0.19, 0.84}	0.0032 (0.0025, 0.0039) {0.23, 0.54}	0.0025 (0.0020, 0.0030) {0.38, 0.02}	0.0037 (0.0027, 0.0049) {0.19, 0.84}
σ_i	0.002	0.0018 (0.0015, 0.0021) {0.15, 0.60}	0.0018 (0.0015, 0.0021) {0.15, 0.60}	0.0017 (0.0014, 0.0020) {0.17, 0.48}	0.0018 (0.0015, 0.0021) {0.15, 0.62}	0.0018 (0.0015, 0.0020) {0.15, 0.56}	0.0017 (0.0014, 0.0020) {0.16, 0.50}
σ_g	0.004	—	0.0041 (0.0037, 0.0046) {0.08, 0.84}	0.0033 (0.0025, 0.0039) {0.20, 0.52}	—	0.0041 (0.0036, 0.0046) {0.08, 0.84}	0.0033 (0.0025, 0.0038) {0.20, 0.56}
ϕ_π	2.0	2.11 (1.97, 2.24) {0.07, 1.00}	1.92 (1.67, 2.25) {0.09, 1.00}	2.08 (1.87, 2.34) {0.08, 0.94}	2.10 (1.97, 2.24) {0.07, 0.98}	1.92 (1.66, 2.27) {0.09, 0.98}	2.08 (1.86, 2.32) {0.08, 0.96}
ϕ_y	0.5	0.39 (0.26, 0.53) {0.26, 1.00}	0.53 (0.34, 0.70) {0.22, 0.98}	0.52 (0.30, 0.69) {0.23, 1.00}	0.39 (0.27, 0.52) {0.27, 1.00}	0.53 (0.34, 0.70) {0.22, 0.98}	0.52 (0.30, 0.68) {0.23, 1.00}
Σ		1.87	1.92	2.12	1.86	1.91	2.12

Table 7: Average, $(5, 95)$ percentiles, and $\{\text{NRMSE}, \text{CR}\}$. Σ is the sum of the NRMSE across the parameters.

REFERENCES

ARUOBA, S., P. CUBA-BORDA, AND F. SCHORFHEIDE (2018): "Macroeconomic Dynamics Near the ZLB: A Tale of Two Countries," *The Review of Economic Studies*, 85, 87–118, https://doi.org/10.1093/restud/rdx027.

GORDON, N. J., D. J. SALMOND, AND A. F. M. SMITH (1993): "Novel Approach to Nonlinear/Non-Gaussian Bayesian State Estimation," *IEE Proceedings F - Radar and Signal Processing*, 140, 107–113, https://doi.org/10.1049/ip-f-2.1993.0015.

GUERRIERI, L. AND M. IACOVIELLO (2017): "Collateral Constraints and Macroeconomic Asymmetries," *Journal of Monetary Economics*, 90, 28–49, https://doi.org/10.1016/j.jmoneco.2017.06.004.

HERBST, E. P. AND F. SCHORFHEIDE (2016): *Bayesian Estimation of DSGE Models*, Princeton, NJ: Princeton University Press.

KITAGAWA, G. (1996): "Monte Carlo Filter and Smoother for Non-Gaussian Nonlinear State Space Models," *Journal of Computational and Graphical Statistics*, 5, pp. 1–25, https://doi.org/10.2307/1390750.

KOOP, G., M. H. PESARAN, AND S. M. POTTER (1996): "Impulse Response Analysis in Nonlinear Multivariate Models," *Journal of Econometrics*, 74, 119–147, https://doi.org/10.1016/0304-4076(95)01753-4.

KOPECKY, K. AND R. SUEN (2010): "Finite State Markov-chain Approximations to Highly Persistent Processes," *Review of Economic Dynamics*, 13, 701–714, https://doi.org/10.1016/j.red.2010.02.002.

ROUWENHORST, K. G. (1995): "Asset Pricing Implications of Equilibrium Business Cycle Models," in *Frontiers of Business Cycle Research*, ed. by T. F. Cooley, Princeton, NJ: Princeton University Press, 294–330.

SIMS, C. A. (2002): "Solving Linear Rational Expectations Models," *Computational Economics*, 20, 1–20, https://doi.org/10.1023/A:1020517101123.

STEWART, L. AND P. MCCARTY, JR (1992): "Use of Bayesian Belief Networks to Fuse Continuous and Discrete Information for Target Recognition, Tracking, and Situation Assessment," *Proc. SPIE*, 1699, 177–185, https://doi.org/10.1117/12.138224.